J. Astrophys. Astr. (2015) **36,** 81–101

Temporal Variation of Ca–K Line Profile of the Sun during the Solar Cycle 22 and 23

G. Sindhuja[1,2,*] & Jagdev Singh[1]
[1]*Indian Insititute of Astrophysics, Koramangala, Bangalore 560034, India.*
[2]*Mangalore University, Mangalagangotri, Mangalore 574 199, India.*
[*]*e-mail: sindhuja@iiap.res.in*

Received 24 September 2014; accepted 8 December 2014

Abstract. We obtained the Ca–K line profile of the Sun as a star since 1969 at the Kodaikanal Observatory (KO) and analysis of the data showed the need to delineate the role of different chromospheric features to the variations of solar irradiance. We, therefore, initiated a new methodology to make observations of Ca–K line profiles of the Sun as a function of latitude and integrated over the longitude on a daily basis since 1986. We have collected the data for about thousand days, spread over two solar cycles. Earlier data (before 1997) were recorded on the photographic film and later data using the CCD detector. The photographic film data were digitized and analysed along with the data obtained from CCD camera. From these data, we computed K_1 and K_2 widths for the Sun as a star, using all the observed line profiles as a function of latitude. In addition, we have analyzed the spectra of the whole Sun as a star obtained on some days and compared it with the results obtained from latitude spectra of the same day. The K_1 and K_2 widths of the Sun as a star derived from the KO data are compared with values determined from the observations made at other observatories to compare results from the new methodology of observations adopted by us and the earlier techniques. The average values of K_1 width during the minimum period. of solar cycle 23 are smaller than those during the minimum period of cycle 22. Day-to-day variations in the K_1 and K_2 widths and plage areas may imply that irradiance variations occur not only due to large-scale solar activity, but also because of variations in some of the three types of network in quiet regions of the Sun. The variation in intensity of the plages can also cause day-to-day variations in widths.

Key words. Sun—activity—chromosphere.

1. Introduction

The study of causes of variation in solar irradiance are very important to understand the changes occurring in the earth's climate and weather. Total irradiance variations of the sun occurs on time scales of less than a day to solar cycle, and very large

periods such as centuries. Approximately 60% of the changes observed in TSI between solar minimum and maximum is produced by the UV part of the spectrum less than 400 nm (Solanki & Krivova 2006). The Ca–K index varies by about 18% during the solar cycle (White & Livingston 1981) and the amplitude of total irradiance variation measured radiometrically between minimum and maximum is only ∼0.1% (Fröhlich & Lean 1998). The observations made during the period of 1981 to 1985 shows that the contribution of the UV part of the spectrum to the total solar irradiance (TSI) is 19% (Lean 1989). The large variations in solar irradiance observed during maximum phase could be caused by the faculae brightness over large areas, which compensates the less radiation emitted from sunspot areas (Froehlich *et al.* 1991; Pap *et al.* 1997).

The spectroscopic and photometric observations of the chromosphere in the Ca–K line will be very valuable because of strong correlation between areas of Ca–K emission and photospheric magnetic field (Nindos & Zirin 1998; Ortiz & Rast 2005). The measured area of plages, active network and network depends on the intensity contrast of the features, threshold intensity value, etc., which varies due to day-to-day variations in the sky conditions. Thus, there is always an uncertainty involved in identifying the extent of various features reliably (Worden *et al.* 1998; Tlatov 2009; Foukal *et al.* 2009; Ermolli *et al.* 2009; Priyal *et al.* 2014) and determining their contribution to the variation in solar irradiance with time from the Ca–K images of the Sun. In addition, the intensity of different Ca–K plages is likely to be different, due to magnitude of underlying magnetic field, and may vary with time or solar cycle phase. Therefore, the determination of irradiance from the areas of features has some uncertainty, whereas measurements from the spectroscopic observations, variations in both the intensity and areas are considered automatically. In order to overcome this problem, Bappu (1974, personal communication with Singh) started monitoring the Ca–K line profiles of the Sun as a star since 1969 to study the variation in Ca–K line emission with greater confidence. Further, the line profiles are normalized to the continuum or calibrated known intensity at a given wavelength to account for the day to day variations in sky transparency and any change in the instrumental setup. The observations of the Ca–K line profiles of the Sun as a star were also started by other groups around the world (White & Livingston 1978; Oranje 1983; Keil & Worden 1984). They found that several parameters of the Ca–K line profile varied with solar activity and Ca–K index varied by about 20% over the solar cycle phase.

Skumanich *et al.* (1984) proposed a three-component model of cell, network and plage to explain the observed changes in Ca–K line profile, using the extant laws of limb darkening. They were able to fit the model profile with the observed one by considering the contribution of two components, namely, cell and network during the minimum phase. During the maximum phase, the contribution due to plage component alone was found to be insufficient to explain the observed profile. They, therefore, suggested an addition of excess contribution due to 'active network component' to achieve a good agreement between the model and observed Ca–K line profiles. This assumption explained the existence of extra emission during the maximum phase. But the measurements made over the centre of the solar disk over a region of $1' \times 3'$ showed no variation with solar cycle phase (White & Livingston 1981; Livingston *et al.* 2007). Hence, it might imply that the extra emission originates from higher latitudes.

The spatially resolved spectra indicate that regions of plages and networks show larger K_1 widths and smaller K_2 widths as compared to quiescent regions (White & Livingston 1981; Bappu & Sivaraman 1971), depending upon the intensity of the features. Also, the emission at the K_{2V} and K_{2R} wavelength regions increases with the intensity of the features. The intensity of plages vary by a large amount and, thus, likely to have large changes in the K_1 and K_2 widths. Enhanced, active and quiet network have also varying contribution of less magnitude to the K_1 and K_2 widths because of less emission from these features. The detailed observations and width measurements of all these spatially resolved features in future may help to model the day-to-day variations. The 'Sun as a star' studies provide important information about solar variability but do not provide sufficient inputs to delineate the contribution of various features to TSI. The variation in polar region has been investigated by counting bright points in the chromospheric images and small scale bipolar regions from magnetograms (Harvey *et al.* 1982; Harvey & Recely 2002; Raouafi *et al.* 2007) which requires support from some other observations. Pevtsov *et al.* (2013), using Ca–K line profiles made the effort to understand the variations of quiet chromosphere by removing K_2 components from the Ca–K line profiles, the resultant of which is also known as basal component. The basal profile originates from non-magnetic chromosphere and showed slight variation between minimum and rising phase of the sunspot cycle. It may be possible that the contribution of 'active network' component introduced by Skumanich *et al.* (1984) comes from different latitudes at different times, probably due to spread of decaying magnetic fields or some other reasons. To estimate the contribution of the active network component to chromospheric irradiance, a new technique of observations was developed by Singh in 1986, Singh (1989) at Kodaikanal Solar Tunnel Telescope, which involves taking the spectra around the Ca–K line as a function of latitude and integrated over the visible 180° longitude. Singh *et al.* (2004) analysed data of 2 years (1986–1987) of the Ca–K line profile as a function of latitude and made initial study to determine the contribution of plages and network flux to the line width. This methodology also helps to study the variations in polar regions with time confidently. Hence, we have collected the data on a day-to-day basis covering about two solar cycles. In this paper, we studied the variations in the Ca–K line profiles of the Sun as a star and compared the results with the results obtained by White & Livingston (1978) and Keil & Worden (1984), to establish the authenticity of our method of observations. In the next section, we provide the details of observations at Kodaikanal using high-resolution spectrograph and calibration of the data. The results and the intercomparison with other observations is described in Section 4. The paper ends with a summary of the results and discussions.

2. Observations

To study the long-term variability of the solar chromosphere, Ca–K line profiles of the Sun as a star were obtained using high-resolution spectrograph at a number of observatories around the world (White & Livingston 1978; Keil & Worden 1984; Sivaraman *et al.* 1987) adopting different procedures to obtain the Ca–K line profiles. In the initial stage, the methodology adopted at Tower Tunnel Telescope, Kodaikanal observatory (KO) to take spectra of the Sun as a star, was to cover the third mirror of

the three mirror coelostat system by a metal cover painted with white pigment (TiO_2) that scatters the radiations with high efficiency. The spectra of the Sun as a star covering a spectral range of about 10 Å around the Ca–K line were recorded using a Kodak 103-aO, 35 mm film with a large exposure time in the range of 120–180 minutes.

On a number of days, the integrated spectrum remained underexposed because of appearance of clouds while recording the spectrum, as a large exposure time was required due to large reduction of intensity at the spectrograph slit because of painted cover on the third mirror. To decrease the exposure time from couple of hours to couple of minutes, the third mirror was kept uncovered and the removal of objective lens from the beam path enabled every point on the slit to receive light from the whole of the Sun, as the first mirror subtended an angle more than half a degree on the slit.

Apart from these, we also obtained the spectra of the Sun in the Ca–K wavelength as a function of latitude integrated over the longitude (starting from 1986 to 2011) in the following way: (1) A portion of the Sun's image is allowed to pass through the slit of the spectrograph. (2) While the Sun's image is moved with uniform speed from East end to the West end on the slit of the spectrograph at a particular latitude, the spectra in the Ca–K wavelength is obtained. (3) The procedure is repeated for each 10° latitude belt, but the spectra is integrated over the longitude belt.

An objective lens of 38 cm diameter of 36.6 m focal length forms an image of the Sun of 34 cm diameter at the slit of the spectrograph. The 18.3 m focus spectrograph with Littrow arrangement using a 600 lines/mm grating blazed at 25000 Å at the first order, provides a dispersion of 9.34 mm/Å around the Ca–K line in 6th order. The slit width (0.1 mm) of the spectrograph is maintained throughout the observing period. This provides the uniformity in the instrumental line profile whose width is much smaller (about 11 mÅ) as compared to the Ca–K line. The 50 mm length of the slit covers about 16° near the equator but the 35 mm 103-aO Kodak film used to record the spectra covers less range in latitude.

To obtain the spectra as a function of latitudes, we made the sunchart on a thick sheet of paper, whose size corresponds to the size of the Sun's image and the center is located at B_0 angle. Each sunchart can be used for about 5 days when the B_0 angle varied with time relatively faster, and for about 20 days when the B_0 varied slowly. The latitude lines at an interval of 5° are drawn on the sunchart. The sunchart is kept near the focal plane of the Sun's image in such a way that N–S axis marked on the sunchart becomes parallel to the axis of rotation of the image. The height of the sunchart is adjusted in such a way that when the North limb of the Sun's image is moved along a particular latitude line (say 30°N) on the sunchart, the same latitude area of the solar image (30°N) falls on the centre of the slit. To integrate the spectrum over the 180° longitudes at that latitude, the image is moved in the E–W direction of the Sun along the given latitude line at a uniform speed by moving the second mirror of the coelostat with the help of an electric motor. After taking the 17 spectra covering all the latitudes of the Sun with an interval of 10° each, 5 calibration spectra with step wedge having 6 different density steps were taken with different exposure times (5 – 30 s) in the nearby continuum to cover larger density range. In addition to this, a spectrum of the Sun as a star around the Ca–K line was obtained as explained above.

All the spectra were recorded on 35 mm Kodak 103-aO film till February 1997. The 103-aO film being used to record the spectra became unavailable and we procured a CCD camera of 1K × 1K format from Photometrics in 1997. A smaller CCD chip size of 24.6 mm × 24.6 mm, as compared to the width of 35 mm film, restricted the spatial and spectral coverage of the spectrum. In case of CCD, to overcome the limitation of spectral coverage, the spectrum around the Ca–K was taken in the 5th order, and spectra near the equator with a latitude interval of 5° to cover all the latitudes of the Sun. The 35 mm 103-aO Kodak film used to record the spectra covers about 11° in latitude near the equator and about 30° near the polar regions. Therefore, spectra were obtained at an interval of 10° latitude to cover whole of the Sun. The shadow caused by a wire kept in front of the spectrograph slit serves as the reference to mark the latitude position on the spectra. The CCD chip is of smaller size and covers about 7° in latitude near the equator and about 20° near the polar region. Hence, we obtained spectra at an interval of 5° latitude up to 30° latitude, and at an interval of 10° beyond 30° latitude. Later, the spectra were combined to study the Ca–K line profiles averaged over 10° latitude at an interval of 10° to maintain the uniformity throughout the period. Twenty three spectra at different latitudes and one spectra of the Sun as a star were obtained daily, sky conditions permitting. On a number of days, spectra around the Ca–K line were also obtained as a function of longitudes during the minimum phase of the Sun, to compare line parameters at the different latitudes with those of longitudes, respectively.

The use of CCD camera necessitated to take the dark and flat field images to correct for the dark signal and pixel-to-pixel gain variations. We used the overlapping 3rd order continuum around 6000 Å for the flat field images using 8 mm slot instead of the slit, and defocused solar image. In the year 1999, the CCD camera from Photometrics was replaced by the CCD camera of 2K × 2K format from ANDOR company, having higher efficiency in the UV and smaller pixel size of 13.5 × 13.5 microns. Sometimes, when ANDOR camera was required for other purposes, Photometrics camera was used to make the observations. This way, we have collected the spectral data around the Ca–K line since 1986.

3. Data analysis

The 23 years of data starting from 1989 to 2011 have been used to study the line width variation over the solar cycle. Most of the observations are made during the months of December to May, as the period from June to November is mostly cloudy, due to the monsoon at Kodaikanal observatory. Observations were made on 1205 days during this period of 23 years, but we found the data of 807 days to be useful for the study, other days of data sets were not complete or had calibration problems. In Figure 1, we show the distribution of the number of days of data in a year used in this analysis. The data are of three types (i) data obtained using the photographic film, (ii) the data with the CCD camera with pixel size of 24 × 24 microns; and (iii) spectra obtained with CCD camera having pixel size of 13.5 × 13.5 microns.

To study the effect of 3 different detectors in the data, first we computed the pixel resolution in each case and found that the values of dispersion per pixel are in the range of 0.0035–0.0046 Å, better than the resolution due to the slit width (0.011 Å). In Figure 2, the normalized Ca–K profiles averaged over two spatial intervals indicate

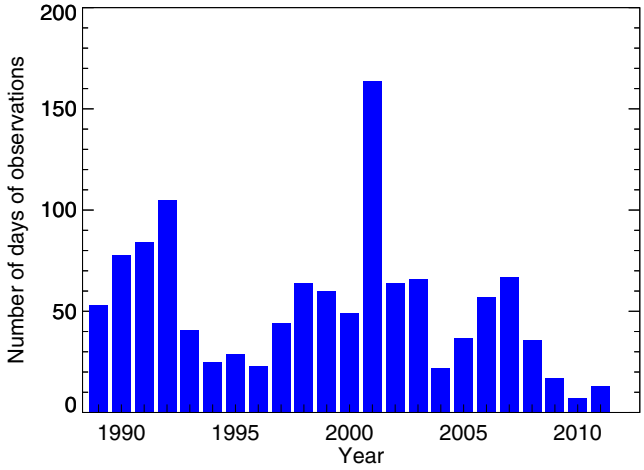

Figure 1. The histogram indicates the number of days the observations were made each year.

small scale variations in the average profile for shorter interval of 0.25°, caused by dust particle or some other irregularity on the detector. These variations are averaged out in the average profile over 10° that is being used to derive the line parameters.

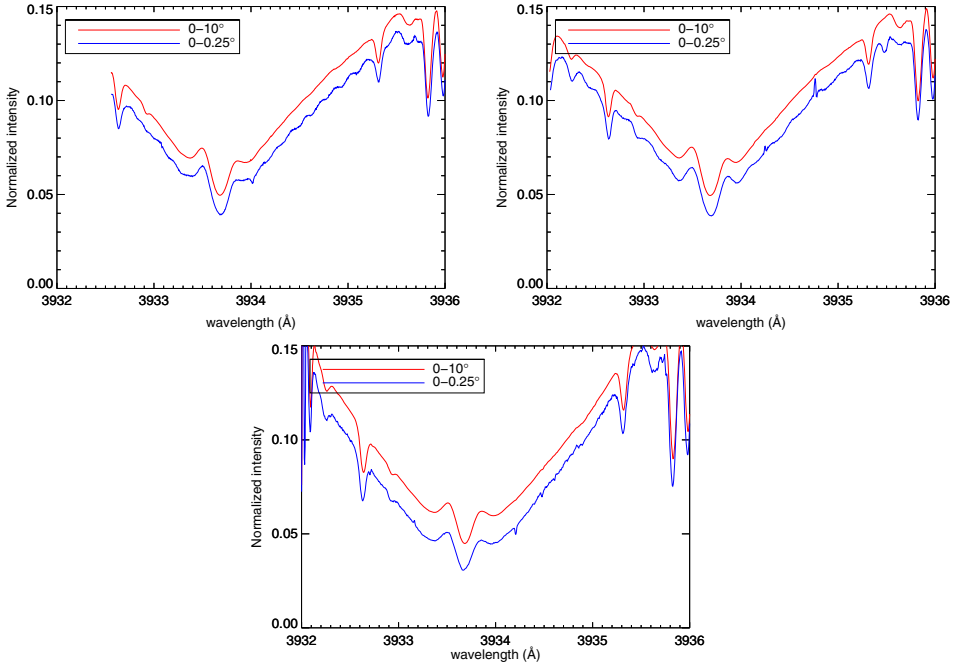

Figure 2. The figure shows the averaged Ca–K line profiles for the 0.25 and 10° spatial intervals for the three types of detectors used. The intensity values of 0.25° intervals have been decreased by 0.02 to separate out two line profiles. *Top left*: Data taken on 2006 March 15 using photometrics CCD, *top right*: data taken on 2005 March 22 using Andor CCD, *bottom*: data taken using the photographic film on 1994 January 5.

Table 1. Comparison of the data obtained with three different detectors.

Detector	Year of observation	Pixel resolution in Å	Rms variation in average profile over	
			0–10°	0–0.25°
Photographic film	1989–1996	0.0046	1.6e–04	5.4e–04
Photometrics	1997–1999	0.0035	7.7e–05	4.8e–04
Andor	2000–2011	0.0039	2.3e–04	2.1e–04

Then, to determine the rms variations in the line profile, we choose an interval of 3933.13–3933.27 Å, where the intensity variation appears to be linear with wavelength. After normalization of the line profiles, the residual intensity is around 0.08. In Table 1 we list the pixel resolution, rms variation computed after subtracting the linear variation with wavelength for the average line profiles over 0.25° and 10° latitudes. Similar values of pixel resolution and rms variations in the line profiles, as listed in Table 1, indicate that the change in detector may not have any effect on the derived line parameters. In the following, we describe the methodology used to do the initial analysis for each set of data.

3.1 *Analysis of photographic film data*

To convert the analog photographic data, to digital data we developed a digitizing unit using a uniform light source. A good camera lens is used to avoid any vignetting in the spectral data. The CCD camera used in the digitizing unit has pixel of 13.5×13.5 microns size with 16-bit read out. The unit was dedicated to digitize this data to maintain the same magnification and uniformity. All the data were digitized under uniform environment conditions. The data are corrected for the dark current and pixel to pixel variations of the CCD camera used. Software was developed to analyse the data in the semi-automatic mode.

3.2 *Conversion of density to intensity values*

For the photographic data, to convert density values to intensity values, we used 5 step wedge (each step with known percentage of transmission) calibration spectra taken on each day with different exposure times. This method generates a large range of density versus intensity values. We chose continuum portion of the spectra and determined the average value of density for each step and exposure. Following the standard procedure of multiple exposures, we plot these values of density versus intensity as shown in Figure 3. A three-degree polynomial fit is found to represent the best fit to density versus intensity values. The coefficients for the polynomial fits were computed for each day of observations. The intensity values were computed for each spectra to determine the various parameters of Ca–K line. In Figure 4, the left panel shows the observed spectrum and the right panel shows the spectrum after density to intensity conversion.

3.3 *Determination of parameters of Ca–K line*

The data obtained with the CCD camera was corrected for the dark current and the pixel-to-pixel gain variations. Reference spatial position corresponding to the given

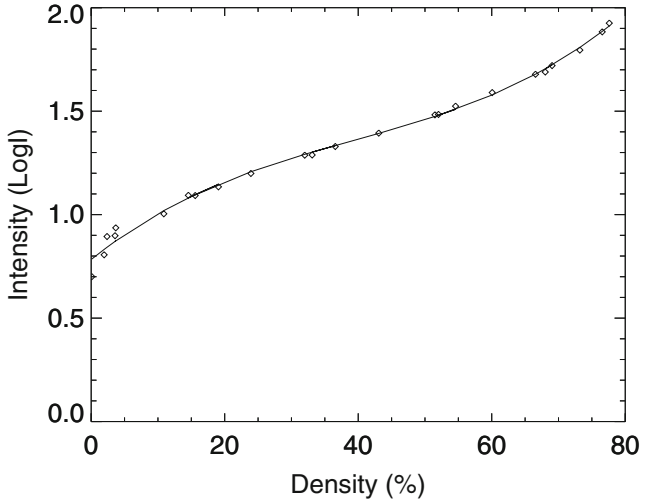

Figure 3. The plot shows density versus intensity values for the data taken on 1997 January 20, along with a polynomial fit (solid line).

latitude on the photographic spectrum, and pixel position on the observed spectrum with the CCD camera were determined. The image size of the Sun and the B_0 angle of the Sun varies with time and, thus, the extent of the interval between two latitudes varies. We computed the Ca–K line profile parameters at an interval of 10° latitude up to 70° latitudes in the northern and southern hemispheres. For the polar regions, we computed the Ca–K line profile parameters averaged over about 20° latitude starting from 70° to the limb of the Sun.

In order to find out the number of spectra to be added in the spatial direction, and to obtain the average spectra at each latitude interval, we adopted the following procedure. The distance of the various latitudes and at the meridian, at an interval of 10°, was computed with respect to centre of the Sun. This has been done by considering the actual size of the solar image on that day. Knowing the radius of

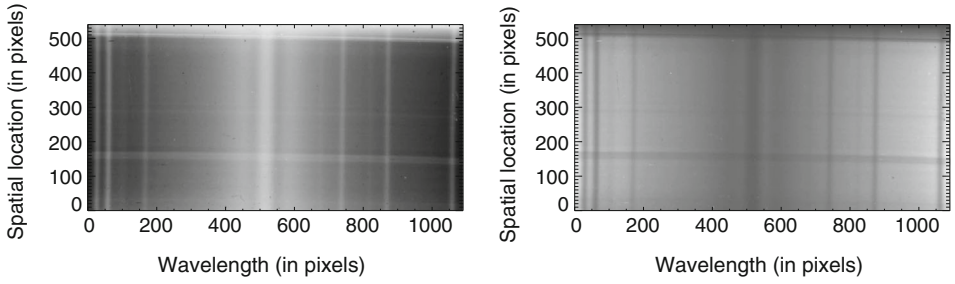

Figure 4. *Left*: Typical observed spectrum taken on 1997 January 20 after the dark and flat-field correction. *Right*: The same spectrum in the intensity values obtained using the coefficients of polynomial fit for that day.

the Sun, the distance (D) between the two latitudes (say θ_1 and θ_2) is computed as

$$D = R^*(\sin\ \theta_1 - \sin\ \theta_2).$$

Then, we computed the number of spectra rows to be added to obtain the average spectrum at each latitude interval. For wavelength calibration of the averaged spectra, we used two photospheric absorption lines of Fe I at 3932.640 Å and 3935.825 Å. The observed intensities were normalized using the residual intensity at 3935.16 Å on the red wing of the Ca–K line. This has been done as 13% of the continuum intensity of the photometrically calibrated Ca–K line profile (White & Suemoto 1968).

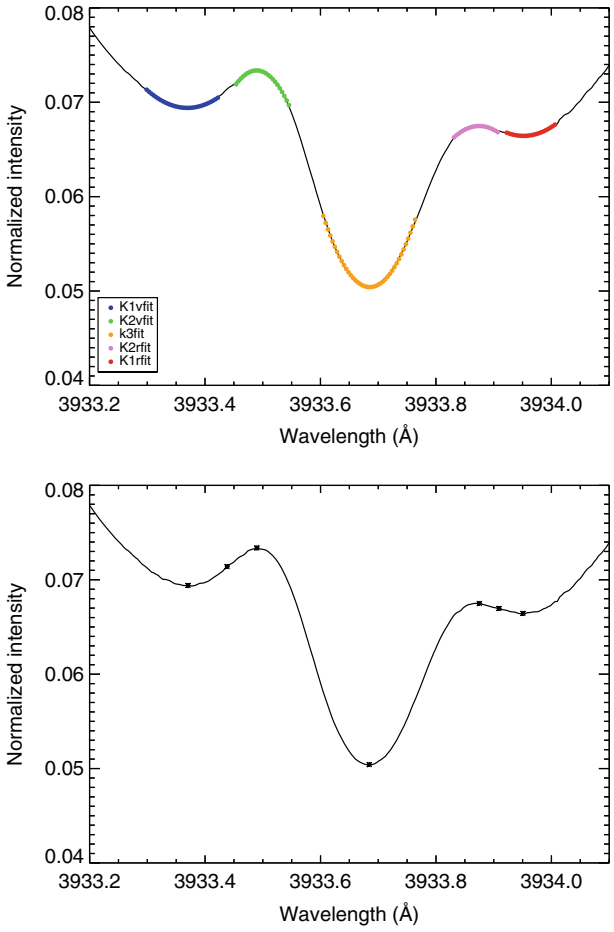

Figure 5. The solid line in both the panels show a normalized averaged observed Ca–K line profile taken on 2007 March 8 for 0–10° south latitude and integrated over the 180° longitude. *Top*: The chosen intervals selected to find the Ca–K line parameters K_{1v}, K_{2v}, K_3, K_{2r} and K_{1r} are plotted with the values obtained from the 3-degree polynomial fit in different colors. *Bottom*: The crosses (stars) marked on the normalized average Ca–K line profile indicate the maxima and minima locations computed from the polynomial fits and the locations to derive the Wilson–Bappu width of the line.

In Figure 5, the solid line shows a typical normalized average Ca–K line profile for the 0–10° latitude interval. The top panel of Figure 5 indicates that the Ca–K line profile has double reversal, and the occurrence of alternative minimum and maximum are known as K_{1v}, K_{2v}, K_3, K_{2r} and K_{1r} locations on the Ca–K line profile. To determine the position and intensity values of these maxima and minima at the Ca–K line profiles, we have carefully chosen 5 small wavelength intervals. These intervals consist of 20–50 points around the maximum and minimum locations, without any cross-talk with the adjacent interval. A large number of points were chosen to accommodate the shift in the minimum and maximum locations in the profiles of different latitudes as the K_1 width is larger at higher latitudes compared with that for lower latitudes. Even though locations of the minima and maxima vary on the line profile with latitude, the chosen intervals are valid for all the line profiles at all the latitudes. We made an attempt to determine the minimum and maximum locations by three methods, namely: (i) comparing the adjacent values, (ii) Gaussian fit, and (iii) 3-degree polynomial fit to each interval. The first and third methods were found to be suitable as compared to the Gaussian fit, because of asymmetry in the profile. To avoid the weightage on a single point, we chose to use a 3-degree polynomial fit method to locate the minimum and maximum as seen in the top panel of Figure 5. The rms value of the difference in line-width measurements from the first and third method is about 0.002 Å for the spectra up to 60° latitudes, and 0.004 Å for spectra greater than 60° latitudes. This is much smaller than the observed variation of 0.169 Å in K_1 and 0.049 Å in K_2 width (see Table 2) with time. In the bottom panel of Figure 5, the location of minima and maxima are shown by crosses along with points to determine the Wilson–Bappu width of Ca–K line. After locating the minima and maxima, we can determine the K_1, K_2 widths of Ca–K line and intensity ratios as defined below:

K_1 width: K_1 width is defined as the wavelength separation between the K_{1v} and K_{1r} minima.
K_2 width: K_2 width is defined as the wavelength separation between the K_{2v} and K_{2r} emission peaks.
Wilson–Bappu width: The wavelength difference of the two wavelength positions corresponding to $(IK_{1r} + IK_{2r})/2$ and $(IK_{1v} + IK_{2v})/2$ gives the Wilson–Bappu width.

Other parameters of interest are the derivation of Ca–K line indices, namely 1 Å and 0.5 Å index, to study the variation in solar radiance with time. Here, we plan to study the line width measurements and its variation with time, the parameters related with the intensity measurements will be investigated separately.

Table 2. Statistics of the line parameters after removal of outliers considering the 2σ level variations.

	Kodaikanal		Kitt peak		NSO/Sac peak	
	K_1 width (Å)	K_2 width (Å)	K_1 width (Å)	K_2 width (Å)	K_1 width (Å)	K_2 width (Å)
Mean	0.633	0.366	0.641	0.369	0.630	0.375
σ	0.039	0.011	0.040	0.010	0.048	0.017
$\text{Width}_{\text{max}} - \text{Width}_{\text{min}}$ (range)	0.169	0.049	0.166	0.039	0.221	0.130
Residual σ	0.022	0.007	0.016	0.005	0.026	0.013

4. Results

We have made observations of the Ca–K line profiles as a function of latitudes and integrated over the visible longitudes on a daily basis for about two solar cycles. The observations made during poor sky conditions and high clouds caused the intensity vignetting in the data. While analysing the data, we found that observations made during poor sky conditions got affected and gave different values of the line parameters. Using the record of sky conditions maintained in the logbook, we discarded all the data obtained on the days with poor sky conditions. Instrumental stray-light also affects the line profile, but the agreement in parameters such as mean, range and standard deviation values for K_1 and K_2 widths for the Kodaikanal, Kitt peak and NSO/Sac peak (Table 2) indicate that scattered light in the instruments have been less or similar to others.

Before we study variations in the Ca–K line profiles with latitude and time, it may be a good exercise to establish the methodology of observations by comparing the results of these observations with the results of similar observations of the Sun as a star carried out at other observatories. We have also made limited observations of the Sun as a star for about 20% of the days compared to the data taken as a function of latitude. For comparison with other observations of the Sun as a star, more data points are desired. We, therefore, planned to determine the average Ca–K line parameters by combining results of observations at all the latitudes and compared these with our observations of the Sun as a star. It is rather difficult to give the weightage factor to Ca–K line profiles of each latitude properly, to combine all the observed profiles on a given day to study the combined profile of the Sun as a star, because of varying intensity due to limb darkening and area with latitude. The comparison of average values of parameters for the Ca–K line and the integrated values for the Ca–K line profiles of the Sun as a star obtained on a number of days will help to determine the factor that needs to be applied to the average value to get the integrated value and thus enlarge the data base.

To begin with, we have considered only two parameters for the comparison, namely, the K_1 and K_2 widths. From the comparison of daily values, it appears that the computed average values of K_1 and K_2 widths are greater than those observed from the Sun as a star. The large values of K_1 and K_2 widths as compared to the Sun as a star values are likely, due to the different weightage factor. We have taken simple average of the K_1 and K_2 widths for all the latitudes whereas, areas at each latitude observed are different, and it is maximum at the equator.

To determine the relation between the average values of K_1 and K_2 widths and observed values of Sun as a star, we made the scatter plots for both of these parameters as seen in the top and bottom panels of Figure 6. The plot of average K_1 width derived from values of all latitude (hereafter referred as average value) versus K_1 width of the Sun as a star (referred as integrated value) is shown in the top panel of Figure 6, which indicates a relation between these two values. We fit a linear and various degree polynomial fits to these data points. The χ^2 test indicated that a quadratic fit matches well to the data points, but it may be noted that linear fit and the quadratic fit yield similar results. From the fit, we derived the relation between the K_1 widths shown in the plot. Using this relation, we computed the integrated values for K_1 widths for each day of observations to make a comparison with other similar observations. We also found that the derived values of K_1 width from the linear and

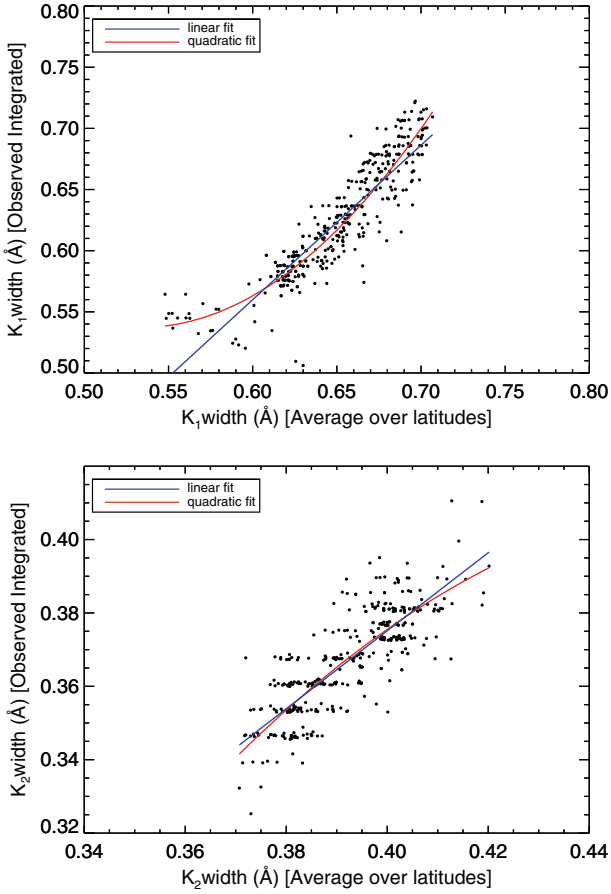

Figure 6. *Top*: Plot of average values of K_1 width derived from the values at all the latitudes vs. values obtained from the observations of the Sun as a star, shown along with linear fits (blue) and quadratic fits (red). *Bottom*: For K_2 width. The χ^2 test indicates that a quadratic fit represents a better relation.

quadratic fits are similar, with a maximum difference of 0.025 Å for the small and larger values of K_1 width. Similarly, we derived the relation for K_2 width as shown in the bottom panel of Figure 6.

4.1 *K_1 and K_2 widths of Ca–K profile and plage areas*

The plages are the brightest among the Ca–K line features and affects the line profiles, relatively, by a larger amount. The emission at K_{2v} and K_{2r} in case of plages is much more than that in the networks. Therefore, variation in plage areas on the sun is likely to cause large variations in K_1 and K_2 widths, as compared to that in the networks. Hence, we have plotted in Figure 7, the K_1 and K_2 width versus plage areas determined from the Ca–K spectro-heliograms obtained at Kodaikanal observatory as described by Priyal *et al.* (2014). The plot shows that generally the K_1 width

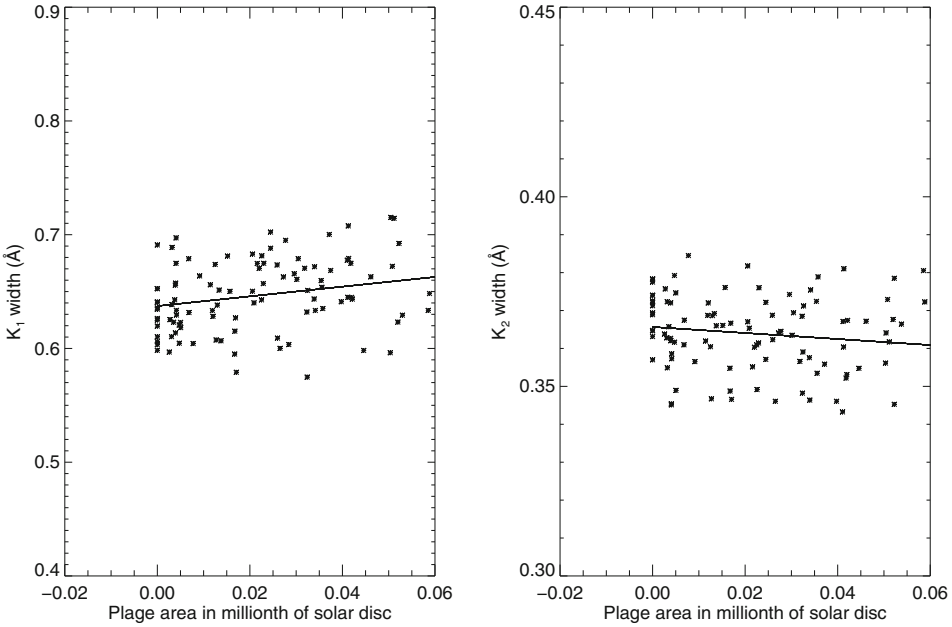

Figure 7. *Left*: Scatter plot of K_1 width vs. measured plage areas in millionth of the solar disc. *Right*: Scatter plot for K_2 width.

increases whereas K_2 width decreases with the increase in plage areas, and the linear fits in the plot confirms the same. The scatter in the plot appears considerable, more than the uncertainty in the measurements of both the parameters. The uncertainty in measurement of width of the K_1 and K_2 is <5 mÅ and the plage areas have been determined fairly well. It appears that plage areas are not able to account for the day-to-day variations in the K_1 width, assuming that intensity is same for all the plages and remains the same during their growth and decay. The scatter can arise because of variations in the contribution of enhanced, active and quiet network towards the K_1 and K_2 widths. Therefore, day-to-day variations in the K_1 width may be due to variations in the contribution from networks, in addition to variation in plage areas. The variation in intensity of plages at shorter time scales as well as solar cycle can also cause variation in K_1 and K_2 widths. The systematic measurements of intensity of plages with time have not been done and considered in modelling the solar irradiance, which may cause day-to-day variations in widths. The K_1 width increases with increasing activity, because higher temperature of active regions is likely to cause broadening of the Ca–K profile. The emission at K_{2v} and K_{2r} also increases in active regions. It is not clear why the K_2 width decreases with increasing activity. It may be due to asymmetry in the profile around K_{2v} and K_{2r} peaks.

4.2 *Comparison of K_1 and K_2 widths with other observatories*

(White & Livingston 1978) and (Keil & Worden 1984) have made extensive observations of the Sun as a star, using Mcmath telescope at Kitt Peak (KP) and NSO/Sac peak observatories, respectively. It may be noted that the observing facility at

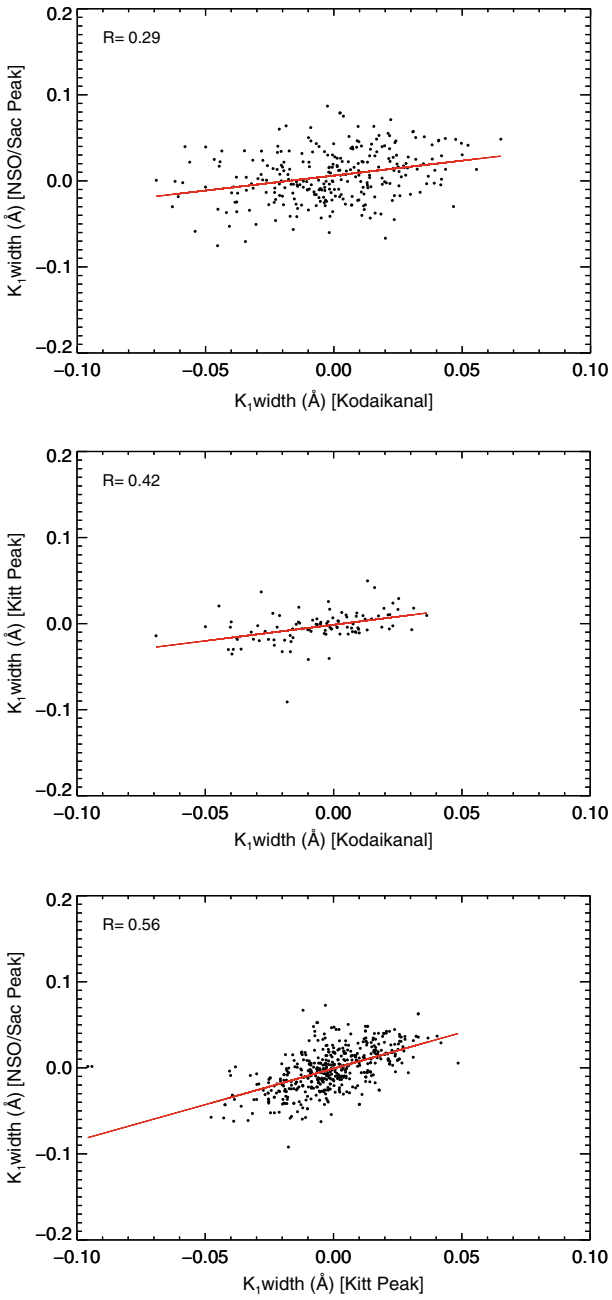

Figure 8. *Top*: The scatter plot of the residual values after removal of outliers and cyclic variations in the measurements of K_1 width for the Kodaikanal data vs. that of NSO/Sac peak data along with a linear fit. *Middle*: Residuals of K_1 width for Kodaikanal vs. Kitt peak. *Bottom*: Data of Kitt peak vs. NSO/Sac peak values along with linear fit. The values of correlation coefficients (R) are written in each panel.

NSO/Sac peak is dedicated to these observations, whereas the facilities at Kodaikanal and Kitt peak are being used for other type of observations too. This caused large gaps and less data sample in KO and KP data as compared to that at NSO/Sac peak observatory. Only 282 days of our observations are common with those of NSO/Sac peak and 100 days of observations are common with those of KP, due to availability of the telescope for this kind of observations and sky conditions. Also, the time difference of about 12 hours exists between our and their observations, due to longitude difference between the locations of the observatories. We have three sets of data, namely, from Kodaikanal, Kitt peak and NSO/Sac peak observatory, but common days of observations are different in these three data sets.

To have a meaningful comparison between the three data sets, first we removed the outliers from all the three data sets by restricting the values up to 2σ level. After removing the outliers from all the three data sets, we computed the mean, standard deviation and difference in maximum and minimum values (range) as listed in Table 2. The mean of K_1 and K_2 widths for all the three data sets are about 0.635 ± 0.005 Å and 0.370 ± 0.005 Å, respectively, indicating a correlation and accuracy in measurements made at all the three observatories. Standard deviation values of K_1 (0.039 ± 0.001 Å) and K_2 widths (0.011 ± 0.001 Å) for KO and KP data are in agreement, as seen in Table 2. But those of NSO/Sac peak differs, being 0.048 and 0.017 Å, respectively. In addition to this, Table 2 indicates that range of values of K_1 and K_2 widths for the KP and KO data agree but differs from the NSO/Sac peak values. Table 2 shows generally an agreement in all the derived parameters, the small differences in values may be due to difference in time of observations. The smaller range and scatter in the width measured at KP and KO as compared to that for NSO/Sac peak values may be because of difference in the resolution of the instruments (5, 6.5, 26 mÅ for the KP, KO and NSO/Sac peak, respectively).

We have chosen yearly mean of the data, due to limited number of observations, to remove the cyclic variation in the K_1 and K_2 widths. Then, we made scatter plots of the residuals of K_1 widths of the Sun as a star for the KO and NSO/Sac peak values (top panel); KO and KP values (middle panel) and KP and NSO/Sac peak values (bottom panel) of Figure 8, to study the correlation between three data sets. The figure shows good amount of scatter in the values, which may be basically due to about 12 hours difference in the observation made on each day. The measurements of widths indicate significant variations in the day-to-day observations. In spite of these factors, there appears correlation between all the data sets, and it may be noted that significance level of the correlation coefficient is above 99% in all the three cases. Further, it may be noted that the mean values of K_1 and K_2 widths determined at KO agrees well with KP than those of NSO/Sac peak with KP. The values of rms variations for the scatter plots of all the three data sets are listed in Table 3. The listed values are close to the resolution limits of observations dominated by the slit

Table 3. RMS variations in the scatter plot of the K_1 and K_2 widths measured for three observatories.

Observatory	K_1 width (mÅ)	K_2 width (mÅ)
Kodaikanal and NSO/Sac peak	28.2	13.7
Kodaikanal and Kitt peak	14.6	4.3
Kitt peak and NSO/Sac peak	20.7	13.7

width of the spectrograph (11 mÅ in case of KO and 26 mÅ for the NSO/Sac peak). Similarly, the residual for the K_2 widths for all the three data sets indicate correlation but, apparently, scatter in the values appear large as seen in Figure 9, because the variations in K_2 widths are much less compared to variations in K_1 width. Further, it may be noted that scatter in the KO and KP values is less than that in the NSO/Sac peak values. Even though the correlation coefficient is small, their significance levels are above 98% in each case. It may be noted that the average amount of scatter is less than the resolution of the instrument for the KO and KP data.

4.3 *Variation of K_1 and K_2 width with solar cycle*

In the upper part of the top panel of Figure 10, we plot the K_1 width of Ca–K line as a function of time (outliers are removed on all the days of observations made between 1989–2011). The sky conditions did not permit the observations during the months from June to November, which caused a gap every year in the plot. Yearly mean values of the K_1 width are indicated by the red dotted solid line in the figure. We also show the Standard Deviation (SD) for the yearly mean by the length of the bar. It may be noted that this is not due to measurement error but because of actual variation in widths caused by variations in Ca–K features such as plages and networks. In the lower part of this panel, residuals of the K_1 width are plotted as a function of time (after the removal of cyclic variations). Similarly, the middle panel of Figure 10 shows the variation of K_2 width and residuals as a function of time. Both these panels indicate that a deviation of residuals are more at maximum and smaller at minimum phase of the solar cycle. These results agree with the finding of Scargle *et al.* (2013). The bottom panel shows the variation in the ratio of K_1 to K_2 width as a function of time. All the three panels indicate large variations in K_1, K_2 and their ratio at short as well as at long time scale, namely days and solar cycle time scales. These might be caused by the rotational modulation or by other phenomena listed by Scargle *et al.* (2013), which cause variations in Ca–K line profile with different amplitude and periods. It is not possible to investigate the short period variations in widths because of large gaps in the data and, hence, we discuss long period variations only. The top panel of Figure 10 indicates that K_1 width of Ca–K line varies with the solar cycle phase, being larger at the maximum phase of the solar cycle and smaller during the minimum phase, apart from the day-to-day variations due to changes in the plage areas. Similarly, K_2 width also varies with the solar cycle phase, but its width is larger at the minimum phase as seen in the middle panel of Figure 10. The ratio of K_1 to K_2 width also varies with the phase of the solar cycle, being larger during the maximum phase of the solar cycle, and it may be noted that the ratio has a lower value during cycle 23 compared to that for cycle 22.

5. Summary and discussions

From the observations of the Sun as a star, White and Livingston (1981) found that K_1 width of the Ca–K line increases with increasing activity, whereas K_2 width decreases. They also reported that K_3 intensity and K-index increases by 30 and 18%, respectively, during the maximum as compared to those at minimum phase of the solar cycle. Worden *et al.* (1998) empirically found intensity threshold values

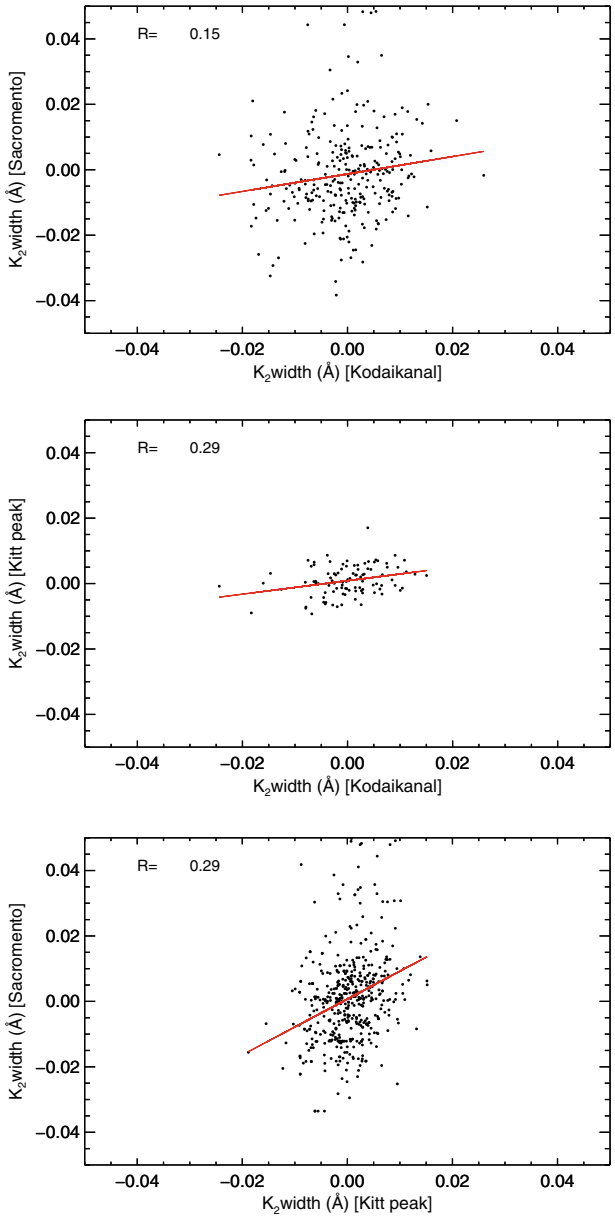

Figure 9. Same as that of Figure 8, but for the K_2 width of the Ca–K line profile.

to identify the Ca–K plages and networks to model the solar irradiance variations. They found that the plage and enhanced network typically cover about 13% and 10%, respectively, of the solar disk around solar-maximum and active network can cover large portion of the Sun during minimum period. Kariyappa and Pap (1996) reported that the variation in spatial index and full width half maximum (FWHM) of the intensity distribution of the chromospheric features such as plages and

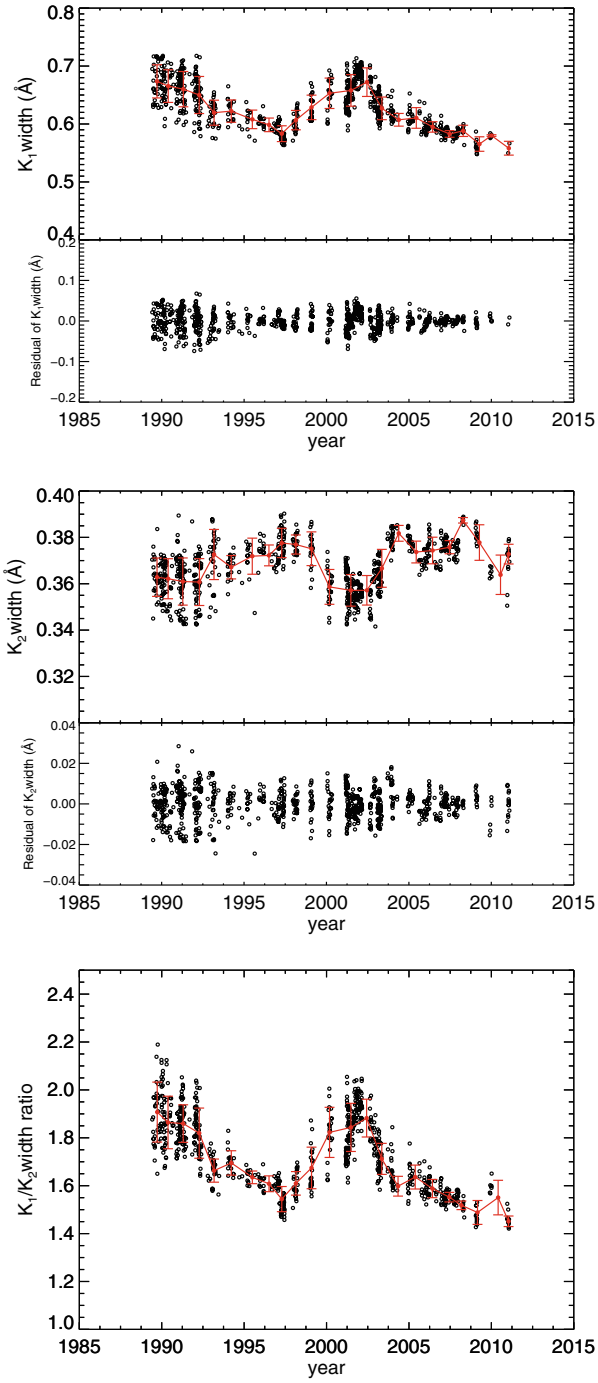

Figure 10. *Top*: Variation of K_1 width with time after outliers removal. *Middle*: Variation of K_2 width with time after outliers removal. *Bottom*: Variation of K_1 to K_2 width ratio with time. The circles show the daily data and the red dotted solid line shows the yearly mean values along with standard deviation.

networks as observed from Ca–K spectroheliograms representing the activity agrees with the UV irradiance measured in MgII h and K lines. Further, Verbeeck *et al.* (2014) and Kumara *et al.* (2014) used segmentation method to identify the active regions, coronal holes and Quiescent Sun (QS) to study the UV and EUV variability of the Sun. Identified active regions are likely to have resemblance with Ca–K plages. The coronal holes cannot be identified in the Ca–K images. The QS identified in EUV images is due to high temperature coronal plasma and the Ca–K emission is because of chromospheric plasma at relatively low temperature. The networks in Ca–K images appears distributed all over the solar surface during all phases of the solar cycle. The boundaries of networks coincide with the boundaries of large convective cells seen in Dopplar-grams (Leighton 1959; Leighton *et al.* 1962) and the contribution to the solar irradiance due to networks vary by few percent with the solar cycle phase (Worden *et al.* 1998). Quiet Sun (QS) identified by Kumara *et al.* (2014) represents solar corona and is the greatest contributor to solar irradiance with up to 63% in the EUV spectral irradiance in terms of intensity. The active regions contribute by about 10% and off-limb features about 24%.

We have made observations of the Ca–K line profiles on a daily basis as a function of latitudes and integrated over the visible longitudes. This data can be used to study the variations in the various parameters with latitude and solar cycle phase for about two solar cycles. The analysis of the data was done to derive the K_1 and K_2 widths of the Sun as a star using the values of K_1 and K_2 widths computed for different latitudes at an interval of 10°. The values of K_1 and K_2 widths of Sun as a star obtained at KO shows good correlation with those obtained at KP and NSO/Sac peak. The results discussed in section 4.1 indicate that the observed day-to-day variations in the K_1 and K_2 widths may be caused by not only the plage areas, but also by variation in intensity of plages and variations in the enhanced, active and quiet networks, and may be responsible for the day-to-day irradiance variations. To delineate the contribution of each feature to these variations, more systematic observations are required. It may be noted that the average value of K_1 width during the maximum phase of the solar cycle 22 is 0.673 Å, and 0.672 Å for cycle 23 (obtained from the yearly mean data). In addition, we find that yearly mean of K_1 width is larger (0.58 ± 0.01 Å) during the minimum phase of cycle 22 for the period of March–December 1997, as compared to the average value (0.55 ± 0.01 Å) during the minimum phase (January–February 2011) of cycle 23. It may be noted that Standard Deviation (SD) is 0.01 Å, whereas the difference in mean values at two minima is 0.03 Å, and large variations are not expected during the minimum phase as seen in the residual plot of Figure 10. Further, the ratios of K_1/K_2 width are 1.54 and 1.45 during the minimum phase of cycle 22 and 23. The smaller value of K_1 width and K_1/K_2 ratio during cycle 23 may be because of the extended minimum phase of this cycle. We speculate that the extended minimum phase may lead to lower temperature of the chromosphere or lower small scale chromospheric activity causing the K_1 width to be smaller as compared to that for cycle 22. The plot of K_2 width versus plage areas indicate that K_2 decreases with increasing activity, but it shows only ∼10% variation in the width as compared to ∼20% variation in K_1 width during these two solar cycles. These findings have support from the fact that in 2010–11, when the sunspot activity has started appearing with sunspot number around 25, the K_1 width continues to be minimum, implying less chromospheric emission in Ca–K. The effect of extended

minimum on the emission in Ca–K line agrees well with the results obtained from the analysis of Ca–K images obtained at Kodaikanal by Singh *et al.* (2012).

Acknowledgements

These observations were planned and started by Jagdev Singh in the year 1986. Jagdev Singh thanks late M. K. Vainu Bappu for introducing him to this subject in 1974 and asking him to observe Ca–K line profiles of the Sun as a star. The authors would like to thank S. Muneer, K. E. Rangarajan, B. Ravindra, K. Sankarasubramanian and S. Krishna Prasad for their valuable inputs and comments and P. Devendran and G. Hariharan for making these observations whenever required. They would also like to thank the referee for useful comments and suggestions.

References

Bappu, M. K. V., Sivaraman, K. R. 1971, *Sol. Phys.*, **17**, 316–330.
Ermolli, I., Marchei, E., Centrone, M., Criscuoli, S., Giorgi, F., Perna, C. 2009, *Astron. Astrophys.*, **499**, 627–632.
Foukal, P., Bertello, L., Livingston, W. C., Pevtsov, A. A., Singh, J., Tlatov, A. G., Ulrich, R. K. 2009, *Sol. Phys.*, **255**, 229–238.
Froehlich, C., Foukal, P. V., Hickey, J. R., Hudson, H. S., Willson, R. C. 1991, in: Solar irradiance variability from modern measurements, edited by Sonett, C. P., Giampapa, M. S., Matthews, M. S., The Sun in Time, pp. 11–29.
Fröhlich, C., Lean, J. 1998, *Geophys. Res. Lett.*, **25**, 4377–4380.
Harvey, K. L., Harvey, J. W., Sheeley, N. R. 1982, *Sol. Phys.*, **79**, 149–160.
Harvey, K. L., Recely, F. 2002, *Sol. Phys.*, **211**, 31–52.
Kariyappa, R., Pap, J. M. 1996, *Sol. Phys.*, **167**, 115–123.
Keil, S. L., Worden, S. P. 1984, *Astrophys. J.*, **276**, 766–781.
Kumara, S. T., Kariyappa, R., Zender, J. J., Giono, G., Delouille, V., Chitta, L. P., Damé, L., Hochedez, J. F., Verbeeck, C., Mampaey, B., Doddamani, V. H. 2014, *A&A*, **561**, A9.
Lean, J. 1989, *Science*, **244**, 197–200.
Leighton, R. B. 1959, *ApJ*, **130**, 366.
Leighton, R. B., Noyes, R. W., Simon, G. W. 1962, *ApJ*, **135**, 474.
Livingston, W., Wallace, L., White, O. R., Giampapa, M. S. 2007, *Astrophys. J.*, **657**, 1137–1149.
Nindos, A., Zirin, H. 1998, *Sol. Phys.*, **179**, 253–268.
Oranje, B. J. 1983, *Astronom. Astrophys.*, **124**, 43–49.
Ortiz, A., Rast, M. 2005, *Mem. Soc. Astron. It*, **76**, 1018.
Pap, J. M., Floyd, L., Lee, R. B., Parker, D., Puga, L., Ulrich, R., Varadi, F., Viereck, R. 1997, in: Long-Term Variations in Total Solar and UV Irradiances, edited by Wilson, A, Correlated Phenomena at the Sun, in the Heliosphere and in Geospace, p. 251.
Pevtsov, A. A., Bertello, L., Uitenbroek, H. 2013, *Astrophys. J.*, **767**, 56.
Priyal, M., Singh, J., Ravindra, B., Priya, T. G., Amareswari, K. 2014, *Sol. Phys.*, **289**, 137–152.
Raouafi, N. E., Harvey, J. W., Henney, C. J. 2007, *Astrophys. J.*, **669**, 636–641.
Scargle, J. D., Keil, S. L., Worden, S. P. 2013, *Astrophys. J.*, **771**, 33.
Singh, J. 1989, *Kodaikanal Obs. Bull*, **9**, 159–164.
Singh, J., Belur, R., Raju, S., Pichaimani, K., Priyal, M., Gopalan Priya, T., Kotikalapudi, A. 2012, *Astron. Astrophys.*, **12**, 201–211.

Singh, J., Gholami, I., Muneer, S. 2004, *Adv. Space Res.*, **34**, 265–268.
Sivaraman, K. R., Singh, J., Bagare, S. P., Gupta, S. S. 1987, *Astrophys. J.*, **313**, 456–462.
Skumanich, A., Lean, J. L., Livingston, W. C., White, O. R. 1984, *Astrophys. J.*, **282**, 776–783.
Solanki, S. K., Krivova, N. A. 2006, *Space Sci. Rev.*, **125**, 25–37.
Tlatov, A. G. 2009, *Sol. Phys.*, **260**, 465–477.
Verbeeck, C., Delouille, V., Mampaey, B., De Visscher, R. 2014, *A&A*, **561**, A29.
White, O. R., Livingston, W. 1978, *Astrophys. J.*, **226**, 679–686.
White, O. R., Livingston, W. C. 1981, *ApJ*, **249**, 798–816.
White, O. R., Suemoto, Z. 1968, *Sol. Phys.*, **3**, 523–530.
Worden, J. R., White, O. R., Woods, T. N. 1998, *Astrophys. J.*, **496**, 998.